



Particle design via powder synthesis: preparation and characterization of $\text{Ba}_{0.5}\text{Sr}_{0.5}\text{Co}_{0.8}\text{Fe}_{0.2}\text{O}_{3-\delta}$ for alkaline water electrolysis

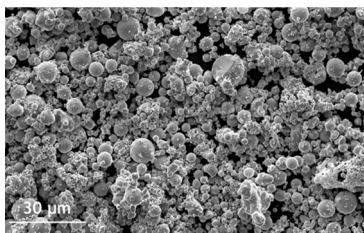
Johannes R. Buchheim¹ · Viktor Drescher¹ · Thorben Vockenber¹

Received: 4 October 2024 / Accepted: 28 March 2025
© The Author(s) 2025

Abstract

The Glatt Powder Synthesis offers a versatile tool for the development and industrial manufacturing of innovative materials for catalyst production. This technology is exemplified by the material $\text{Ba}_{0.5}\text{Sr}_{0.5}\text{Co}_{0.8}\text{Fe}_{0.2}\text{O}_{3-\delta}$ (BSCF), showcasing its application as a catalyst for the Hydrogen Evolution Reaction (HER). The effectiveness of this method is attributed to the specific conditions present in the pulsating hot gas flow.

Graphical abstract



Keywords Spray pyrolysis · Powder synthesis · Catalysts · Heterogenous catalysis · Ceramics

Introduction

Hydrogen is regarded as a key resource for a sustainable energy future and plays a crucial role in the effort to reduce dependence on fossil fuels and lower global CO_2 emissions. The origin of hydrogen is often indicated by a color-coding system that reflects various production methods and their environmental impacts. Green hydrogen, produced through electrolysis using renewable energy sources, is considered the most environmentally friendly option, while blue hydrogen is generated through steam reforming of natural gas with CO_2 capture. In contrast, grey hydrogen has a higher ecological footprint, as it is produced from fossil fuels without CO_2 reduction [1, 2].

Alkaline electrolysis is a central process for producing green hydrogen, wherein water is split into hydrogen and oxygen using electric current. This technology is particularly interesting as it relies on cost-effective catalysts and operates in alkaline media, which can lead to improved efficiency [3]. A critical step in this process is the HER, which is supported by various catalysts. Commonly used catalysts include nickel, platinum, cobalt, molybdenum, and iron, each with their unique advantages and disadvantages [4–6]. Notably, Barium-Strontium-Cobalt-Iron Oxide (BSCF), a mixed oxide, is highlighted for its high catalytic activity and stability in alkaline media, making it a promising catalyst for the HER [7, 8]. The tunability of BSCF's composition allows for the optimization of its properties, leading to enhanced performance in hydrogen production [9].

In this work, the material $\text{Ba}_{0.5}\text{Sr}_{0.5}\text{Co}_{0.8}\text{Fe}_{0.2}\text{O}_{3-\delta}$ is synthesized as a crucial step in the process. This method presents a significant advantage over the traditionally used solid-state reaction, primarily due to its ability to achieve a more uniform particle size and enhanced phase purity. The

✉ Johannes R. Buchheim
Johannes.buchheim@glatt.com

¹ Glatt Ingenieurtechnik GmbH, Nordstraße 12,
99427 Weimar, Germany

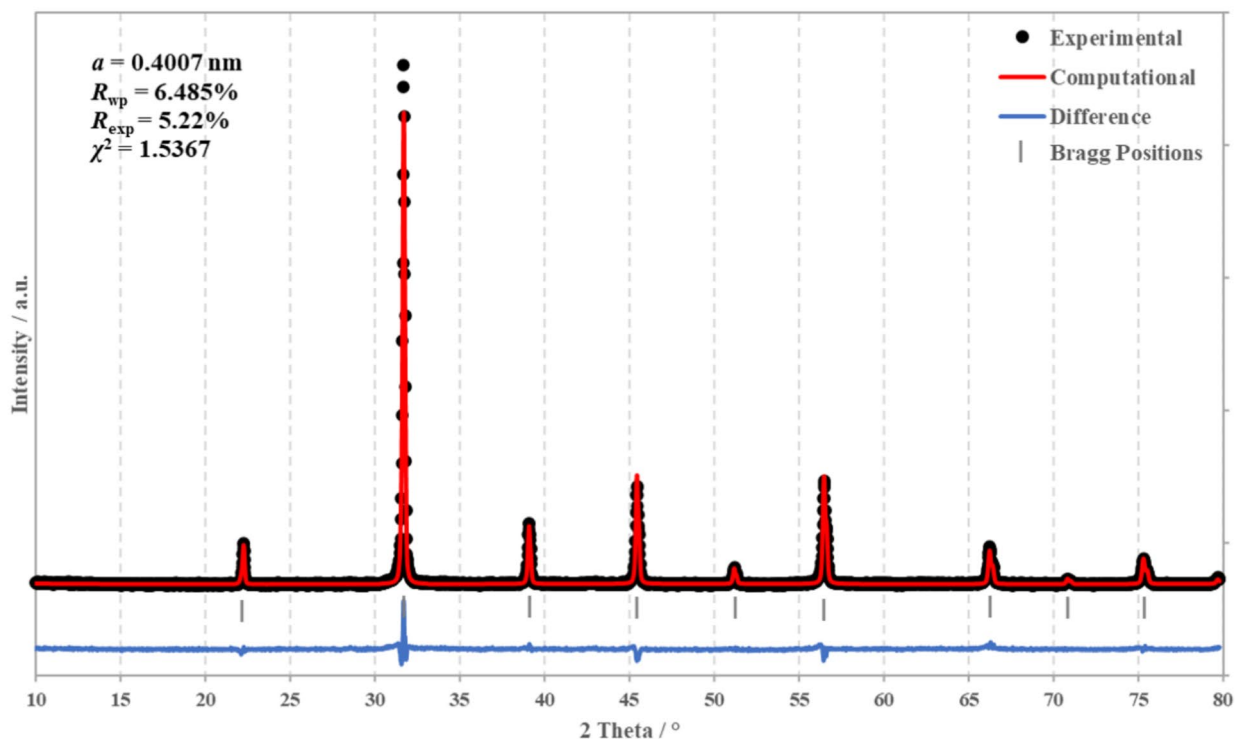


Fig. 1 XRD pattern of the synthesized BSCF

precise control of synthesis conditions in a pulsating hot gas flow allows for improved homogeneity of the final product, which is critical for optimizing catalytic performance. Additionally, the Glatt Powder Synthesis can reduce reaction times and energy consumption, making it a more efficient alternative for producing high-performance catalysts for the HER.

Results and discussion

The synthesis of $\text{Ba}_{0.5}\text{Sr}_{0.5}\text{Co}_{0.8}\text{Fe}_{0.2}\text{O}_{3-\delta}$ was realized by the combustion of a solution containing the stoichiometric amounts of raw materials using the Glatt Powder Synthesis. A comprehensive description of the reactor design is provided elsewhere [10]. The reaction temperature was set to achieve an outlet temperature of $1240 \text{ }^\circ\text{C}$ at the reactor exit. This high temperature is essential for promoting the necessary chemical reactions and ensuring the formation of the desired perovskite structure, critical for the material's effectiveness as a catalyst.

The phase purity of the synthesized BSCF was confirmed using X-ray powder diffraction (Fig. 1). All diffraction lines were found to correspond to the cubic perovskite structure with space group $Pm\bar{3}m$. The sharp lines correspond to

the reflection planes (100), (110), (111), (200), (210), (211), (220) indicating that the material possesses high crystallinity and the desired phase purity. The lattice parameter of the cubic cell was determined via Rietveld structural analysis to be $a = 0.4007 \text{ nm}$, which is consistent with values reported in the literature [11]. The synthesized material is showing isotropic properties with a crystal size of 150 nm . Scanning electron microscopy (Fig. 2) images reveal a spherical morphology with compact and dense particles. The narrow particle size distribution facilitates high packing densities, which is advantageous for catalytic applications, enhancing the overall efficiency of the BSCF catalyst in the HER (Fig. 3).

The polarization curve of the synthesized BSCF was assessed in comparison to glassy carbon and nickel powder. For this purpose, each powder was applied to a rotating disk electrode. The preparation and characterization were based on experimental studies from the literature [11]. The electric potential was corrected for iR losses, ensuring accurate measurement of the electrochemical performance of the materials during the HER (Fig. 4). It can be seen that the prepared BSCF exhibits a high catalytic activity for the HER in alkaline media. Further evaluation of the catalytic activity is to determine the overpotential that is required to deliver an electrode current density of $10 \text{ mA}\cdot\text{cm}^{-2}$ (η_{10}). The prepared BSCF shows a η_{10} of 148

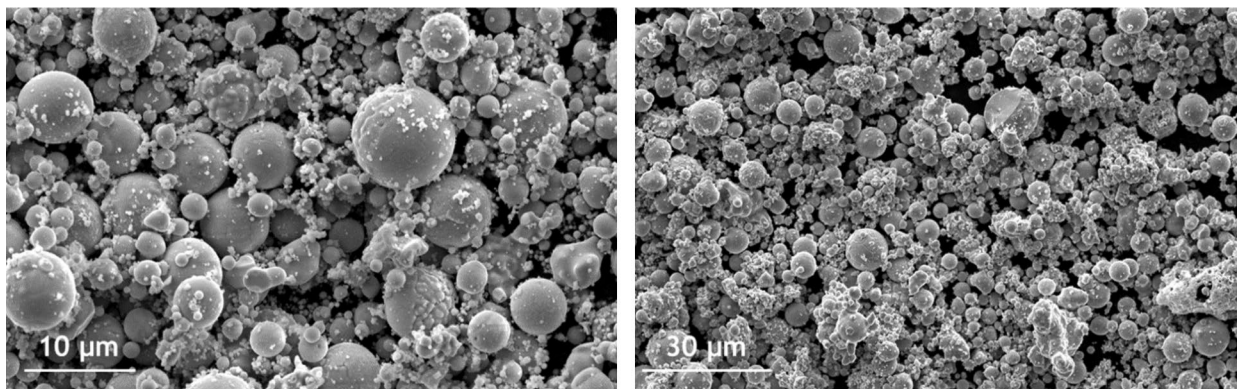


Fig. 2 SEM images of the synthesized BSCF

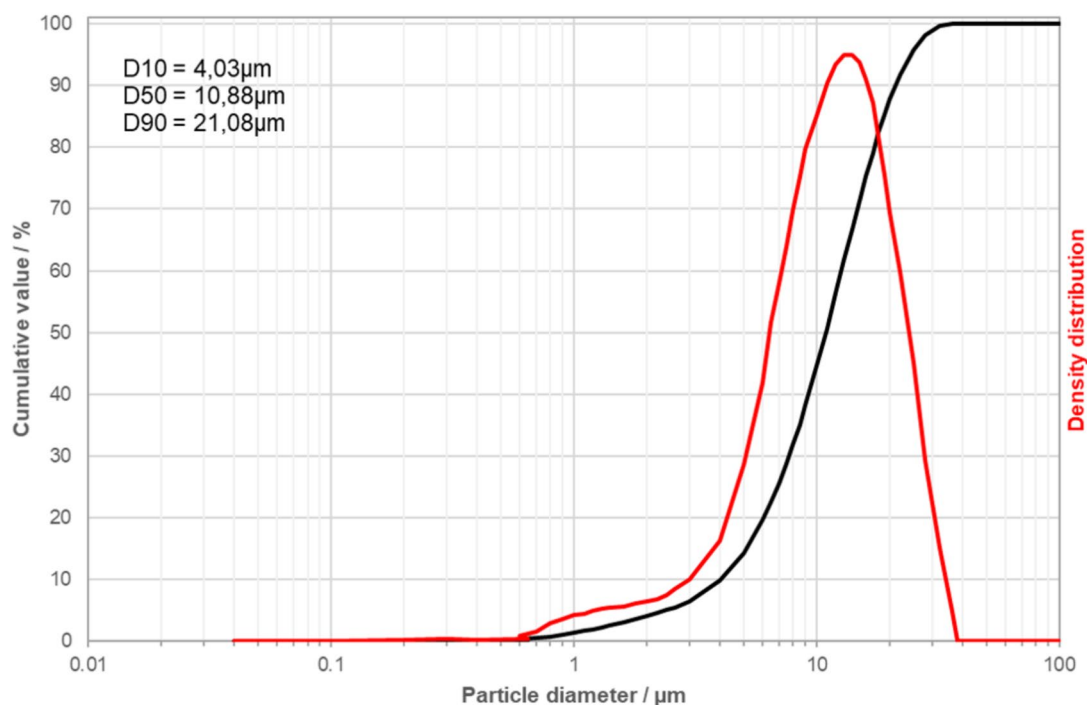


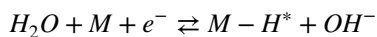
Fig. 3 Particle size distribution of the synthesized BSCF

mV which is significantly lower than the used Ni powder ($\eta_{10} = 485$ mV). The obtained value is comparable to reported overpotentials for several transition metal oxide electrocatalysts including other BSCF materials prepared by other synthesis methods [12, 13].

In alkaline media, HER involves the reduction of water molecules rather than protons, making it kinetically more challenging compared to acidic conditions. The reaction proceeds through two main steps [14, 15]:

1. Volmer reaction

The first step involves the adsorption of hydrogen onto the catalyst (M) surface through the reduction of water:



Here, a water molecule donates a proton, forming an adsorbed hydrogen intermediate ($M-H^*$) while releasing a hydroxide ion (OH^-) into the solution.

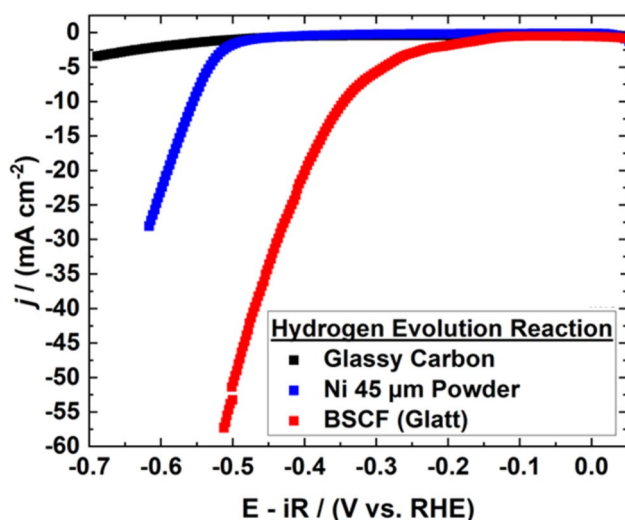
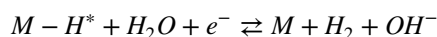


Fig. 4 Electrochemical measurement of HER activity on glassy carbon, nickel powder (45 μm), and BSCF powder

2. Hydrogen evolution pathways

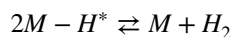
Following hydrogen adsorption, molecular hydrogen is generated via one of two possible routes:

2.1. Heyrovsky reaction (electrochemical desorption)



In this step, the adsorbed hydrogen reacts with another water molecule and an electron to form H_2 , simultaneously releasing an OH^- ion.

2.2. Tafel reaction (hydrogen recombination)

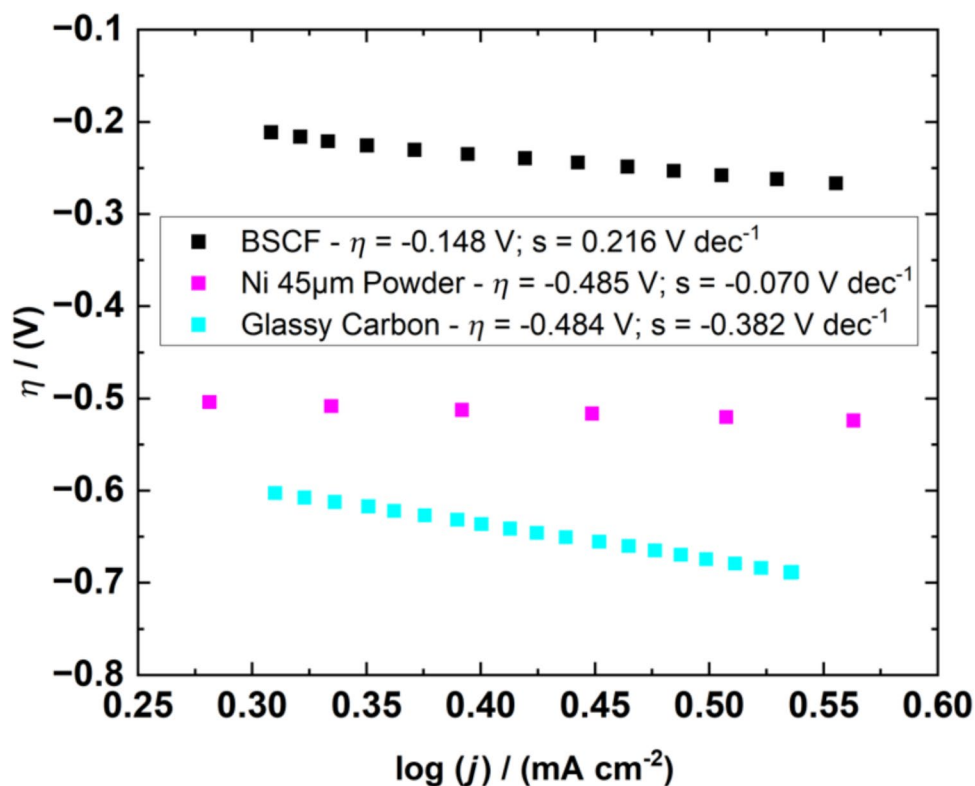


In this mechanism, two adjacent adsorbed hydrogen atoms combine directly to form molecular hydrogen.

To gain a more precise insight into the mechanism involved, Tafel plots were calculated (Fig. 5). The rate-limited step of the HER can be determined by the Tafel slope. Tafel slopes of 120, 40, and 30 $\text{mV}\cdot\text{dec}^{-1}$ give a direction to Volmer, Heyrovsky, and Tafel determining rate steps [14, 15].

The Ni powder shows a Tafel slope of 70 $\text{mV}\cdot\text{dec}^{-1}$ suggesting a mixed Volmer–Heyrovsky mechanism, meaning both H_2O dissociation and electrochemical desorption contribute to the reaction rate. The BSCF materials shows a Tafel slope of 216 $\text{mV}\cdot\text{dec}^{-1}$ which is an unexpected high value for this type of oxide. Typical Tafel slopes are reported between 40 and 120 $\text{mV}\cdot\text{dec}^{-1}$ [12, 13]. This high value could indicate that the HER process is influenced by a combination of slow steps, weak or strong proton adsorption, heterogeneous mechanisms, or even transport and diffusion barriers. For higher values of $\log(j)$ the Tafel slope is only slightly decreasing to a value of 178 $\text{mV}\cdot\text{dec}^{-1}$ which further suggests a complex mechanism.

Fig. 5 Corresponding Tafel plots of glassy carbon, nickel powder (45 μm), and BSCF powder



The catalytic activity of the material may depend on the structural properties, in particular the presence of oxygen defects [12, 16, 17]. Within the crystal lattice, these have an influence on electron transfer. On the catalyst surface, these active sites function for water adsorption and dissociation. A high concentration leads to high activity according to the Volmer mechanism. If the binding of the proton is very strong, the subsequent formation of hydrogen is limited.

A high concentration of defects can lead to a distortion of the surface structure, which in turn changes the catalytic properties of the material. This could lead to the reaction mechanism becoming more complex and additional steps being required. If the defects are not evenly distributed on the surface, this could lead to heterogeneous reaction mechanisms in which different regions of the surface make different contributions to the overall reaction. For the synthesized BSCF material an oxygen defect of $\delta = 0.63$ was calculated that indicates a clear deviation from the ideal ABO_3 structure. A defect density of $\delta = 0.63$ leads to a distortion of the crystal structure, as a considerable proportion of the oxygen positions in the crystal lattice are missing. This distortion can lead to disorder in the material which can be seen by an increase in the lattice constant [18]. The lattice constant of the synthesized BSCF material was calculated with $a = 0.4007$ nm. The increased oxygen defect concentration could possibly be due to the citric acid used as a complexing medium, which has reducing properties, and the high synthesis temperature. The abrupt cooling of the material by cold air freezes these defects.

The distortion of the structure and the resulting defects increase the surface activity, which helps to improve the catalyst performance but could also make the kinetics of the reaction more complex.

Conclusion

This study highlights the successful synthesis of the perovskite material $\text{Ba}_{0.5}\text{Sr}_{0.5}\text{Co}_{0.8}\text{Fe}_{0.2}\text{O}_{3-\delta}$ using Glatt Powder Synthesis, demonstrating its potential as a highly effective catalyst for the HER. The synthesis process, involving the spraying of a stoichiometric solution and maintaining a reactor outlet temperature of 1240 °C, was critical for achieving the desired perovskite structure.

The phase purity of the synthesized BSCF was confirmed using X-ray powder diffraction, with all diffraction peaks corresponding to a cubic perovskite structure. Scanning electron microscopy images revealed a spherical morphology with compact and dense particles, allowing for high packing densities that enhance catalytic performance.

Comparative analysis of catalytic activity showed that BSCF significantly outperforms glassy carbon and nickel powder, making it a promising candidate for alkaline

water electrolysis applications. These findings highlight the importance of optimizing material synthesis to achieve high-performance catalysts that can facilitate the transition to sustainable energy solutions.

Experimental

Synthesis of BSCF oxide

The BSCF oxide was prepared by spray pyrolysis of a solution containing stoichiometric amounts of BaCO_3 , SrCO_3 , CoCO_3 , and $\text{Fe}(\text{NO}_3)_3 \cdot 9\text{H}_2\text{O}$ dissolved in a citric acid solution. First, the carbonates of barium, strontium, and cobalt were dissolved in citric acid solution. Additionally, iron nitrate was added. The molar ratio of cations to citric acid was set to 1.75:1 ($c_{\text{cat}} = 5.4$ mol/dm³). The solution with an oxide content of 30 wt% was sprayed by a two-substance nozzle from the bottom into the reaction chamber using a 2 mm liquid insert and a spray pressure of 3.0 bar. The system was heated up and the spraying process commenced at an outlet temperature of approximately 1220 °C. Due to the exothermic nature of the reaction, the temperature increased to about 1300 °C. The pulse frequency was set to 80 Hz and the spray rate was maintained between 30 and 50 g/min to ensure stability in the outlet temperature at the reactor exit at 1240 °C. The powder was quenched to 120 °C at the reactor outlet using cooling air and was subsequently separated from the process gas stream using an H13 cassette filter.

Material characterization

The phase structure of the BSCF powder was characterized by X-ray diffraction measurement (Phaser D2, Bruker) with a step size of 0.02° in 2θ in the range of 10–70° at room temperature using $\text{CuK}\alpha$ radiation ($\lambda = 1.54065$ Å). Structural information was obtained by Rietveld refinement using Maud software [19]. Background correction was done using a fourth-order polynomial. The images were taken with the Phenom XL scanning electron microscope (Thermo Fisher Scientific) for optical evaluation of the samples. The particle size analyses were performed with the laser diffraction system Cilas 1190 LD (Quantachrome).

Electrochemical measurements

The HER electrochemical activities of the investigated catalysts were evaluated in a three-electrode configuration using a thin film rotating disk electrode system (Pine Research Instrumentation) on an electrochemical workstation (Pine Research Instrumentation) according to preparation and experimental setup find in [11]. A Hg|HgO (1 M KOH) electrode served as the reference electrode, while a graphite

rod acted as the counter electrode. For the preparation of the working electrode, a catalyst ink was formulated by dispersing 5 mg of catalyst material, 1 mg of carbon black, neutralized Nafion into a solvent mixture containing isopropanol and water. The ink was applied onto a polished glassy carbon electrode and allowed to dry while rotating at 700 rpm for approximately 30 min. Before conducting electrochemical measurements, the electrode was preconditioned by cyclic voltammetry in the potential range of -0.9 V to -1.65 V (vs. Hg|HgO) at a scan rate of $100 \text{ mV}\cdot\text{s}^{-1}$ for 40 cycles, with a rotation speed of 1600 rpm. The HER activity was subsequently evaluated through linear sweep voltammetry at a scan rate of $10 \text{ mV}\cdot\text{s}^{-1}$ while maintaining the electrode rotation at 1600 rpm. The electric potential is iR corrected.

Acknowledgements We are grateful to Karl Skadell and Artur Bekisch by Fraunhofer IKTS for the evaluation of catalytic activity of the BSCF sample.

Open Access This article is licensed under a Creative Commons Attribution 4.0 International License, which permits use, sharing, adaptation, distribution and reproduction in any medium or format, as long as you give appropriate credit to the original author(s) and the source, provide a link to the Creative Commons licence, and indicate if changes were made. The images or other third party material in this article are included in the article's Creative Commons licence, unless indicated otherwise in a credit line to the material. If material is not included in the article's Creative Commons licence and your intended use is not permitted by statutory regulation or exceeds the permitted use, you will need to obtain permission directly from the copyright holder. To view a copy of this licence, visit <http://creativecommons.org/licenses/by/4.0/>.

References

- Schneider J, Pischinger S (2021) *Renew Sustain Energy Rev* 135:110133
- Die Nationale Wasserstoffstrategie (2020) German Federal Ministry for Economic Affairs and Climate Action. <https://www.bmwi.de>
- Luo S, Zheng Y, Xu H, Zhang L (2020) *Renew Energy* 155:1153
- Zheng Y, Jiao Y, Chen J (2018) *Chem Soc Rev* 47:7571
- Huang J, Wang S, Wang L, Zhang J (2019) *Mater Today Energy* 12:126
- Matsumoto K, Shibata T, Saito K (2017) *ACS Catal* 7:2056
- Lee S, Kim Y, Park J (2017) *J Mater Chem A* 5:6527
- Gao Y, Chen Z, Wu Y, Zhang X (2020) *Renew Sustain Energy Rev* 119:109576
- Zhou Y, Zhang H, Wang L, Li Y (2019) *J Power Sources* 414:235
- Glatt Ingenieurtechnik GmbH, Weimar, Glatt Powder Synthesis - Thermal treatment of your powders. <https://powdersynthesis.glatt.com/technology/reactors/>; 26 Sep 2024
- Li X, He L, Zhong X, Zhang J, Luo S, Yi W, Zhang L, Hu M, Tang J, Zhou X, Zhao X, Xu B (2018) *Scanning* 134:1608
- Alom MS, Kananke-Gamage CCW, Ramezanipour F (2022) *ACS Omega* 7:7444
- Zhang Z, Zhou W, Yang Z, Jiang J, Chen D, Shao Z (2020) *Int J Hydrog Energy* 45:24859
- Mahmood N, Yao Y, Zhang JW, Pan L, Zhang X, Zou JJ (2017) *Adv Sci* 5:1700464
- Shinagawa T, Garcia-Esparza A, Takanabe K (2015) *Sci Rep* 5:1380
- Lu L, Sun M, Wu T, Lu Q, Chen B, Hei Chan C, Ho Wong H, Li Z, Huang B (2025) *ChemElectroChem* 12:e202400648
- Christy M, Choi S, Kwon J, Jeong J, Paik U, Song T (2025) *Small Sci* 5:2400386
- Zhang C, Bristowe PD (2013) *RSC Adv* 3:12267
- Scardi P, Lutterotti L, Maistrelli P (1994) *Powder Diffr* 9:180

Publisher's Note Springer Nature remains neutral with regard to jurisdictional claims in published maps and institutional affiliations.